Dermatology Practical & Conceptual

Non-Invasive Skin Imaging of Pseudoxanthoma Elasticum Using Dynamic Optical Coherence Tomography: Insights from a Case-Control Study

Camilla Chello[1], Alessandro Laghi[1,2], Ludovica Melchiorri[1], Ilaria Zubba[1], Emanuele Miraglia[3], Marco Ardigò[4,5], Giovanni Pellacani[1], Sandra Giustini[1]

1 Department of Internal Medicine and Medical Specialties, Unit of Dermatology, "Sapienza" University of Rome, Rome, Italy
2 Department of Medicine, Dermatology and STDs Unit, "Celio" Military Hospital, Rome, Italy
3 Dermatology Department, "San Sebastiano" Hospital, Frascati, Italy
4 Dermatology Unit, IRCCS Humanitas Research Hospital, Rozzano, Italy
5 Department of Biomedical Sciences, Humanitas University, Pieve Emanuele, Italy

Key words: Pseudoxanthoma elasticum, Optical coherence tomography, Elastic tissue alterations, Cutaneous imaging, Noninvasive skin assessment

Citation: Chello C, Laghi A, Melchiorri L, et al. Non-Invasive Skin Imaging of Pseudoxanthoma Elasticum Using Dynamic Optical Coherence Tomography: Insights from a Case-Control Study. *Dermatol Pract Concept*. 2025;15(4):5260. DOI: https://doi.org/10.5826/dpc.1504a5260

Accepted: May 19, 2025; **Published:** October 2025

Funding: None.

Competing Interests: None.

Authorship: All authors have contributed significantly to this publication.

Corresponding Author: Camilla Chello, MD, Department of Internal Medicine and Medical Specialties, Unit of Dermatology, "Sapienza" University of Rome, Viale del Policlinico, 155 - 00161 Rome, Italy. ORCID ID: 0000-0002-3142-1831. E-mail: camilla.chello@gmail.com

ABSTRACT

Introduction: Pseudoxanthoma elasticum (PXE) is a rare genetic disorder characterized by progressive mineralization and fragmentation of elastic fibers, leading to multisystem involvement. Diagnosis relies on clinical features, histopathology, and, in selected cases, genetic testing, with cutaneous manifestations often representing the earliest signs.

Objective: To validate dynamic optical coherence tomography (D-OCT) as a noninvasive diagnostic method for detecting PXE-related dermal abnormalities.

Methods: In this case-control study, PXE patients evaluated at Umberto I Policlinic (Rome, Italy) between May 2023 and September 2024 underwent clinical and instrumental assessment. The left lateral cervical, retrocervical, left axillary, and periumbilical folds were analyzed using a standardized 0–3 clinical severity scale and D-OCT imaging. Control subjects were individuals undergoing routine mole checks. D-OCT quantified fiber density, attenuation, and vessel density at 300 µm and 500 µm depths. Statistical analysis included Spearman's correlation and the Mann-Whitney U test, with $p < 0.05$ considered significant.

Results: Twenty-three PXE patients and eleven controls were included. Cutaneous involvement was observed in 91.30% of patients, predominantly in retrocervical (86.95%) and lateral cervical (82.60%) areas. Clinical severity significantly correlated with D-OCT fiber density in the retrocervical region ($\rho = 0.507$). Compared with controls, PXE patients showed reduced fiber density and increased attenuation across most regions, except the axillae. At 500 µm depth, vessel density was markedly decreased in the axillary area, with approximately 2.5-fold fewer vessels in PXE skin.

Conclusion: D-OCT effectively detects dermal alterations in PXE, including subclinical changes, providing a promising noninvasive alternative to skin biopsy.

Introduction

Pseudoxanthoma elasticum (PXE) is an autosomal recessive disorder characterized by mineralization and fragmentation of elastic fibers, leading to symptoms in the skin (papular lesions in flexural areas), eyes (angioid streaks, peau d'orange, subretinal neovascularization, and hemorrhage), and cardiovascular system (peripheral artery disease, gastrointestinal bleeding, ischemic stroke) [1]. It is caused by biallelic pathogenic variants in the ATP (adenosine triphosphate)-binding cassette subfamily C member 6 (*ABCC6*) gene, with over 500 identified pathological variants [2]. Although the precise role of *ABCC6* in PXE pathogenesis remains unclear, it encodes a transmembrane transporter protein that mediates ATP efflux, which is hydrolyzed to inorganic pyrophosphate (PPi) and adenosine monophosphate (AMP). Extracellular PPi provides a potent anti-mineralization effect (which is deficient in PXE), while AMP hydrolysis to inorganic phosphate and adenosine affects cellular properties by modulating the purinergic pathway [3,4].

Currently, PXE diagnosis can be definitive, probable, or possible based on standardized clinical signs, histological features, and *ABCC6* mutational status, although genetic confirmation is not mandatory [5].

The worldwide prevalence of PXE is estimated to be between 1 per 25000 and 1 per 100000, with a female predominance and onset typically in childhood or adolescence [4]. The skin is generally the first affected organ, with flexural surfaces, probably because of the repetitive friction, developing isolated papules or plaques that may coalesce into reticulated plaques, giving a cobblestone appearance [6]. Later, skin laxity and wrinkles may appear [4]. The yellow tone of affected skin, resembling true xanthomas, has led to the name "pseudoxanthoma elasticum" [4].

Specific stains such as Verhoeff-van Gieson for elastin and Von Kossa for calcium deposits can demonstrate short, fragmented, clumped, and calcified mid-dermal elastic fibers in affected skin biopsies [5]. Collagen fibers may also exhibit splitting, thickening, coiling, calcification, and even flower-like deformation [7].

Thus far, studies on PXE cutaneous features have relied on clinical examination, dermoscopy, and histology. However, given that cutaneous manifestations are typically the earliest signs of PXE, noninvasive imaging techniques targeting the dermis such as cutaneous optical coherence tomography (OCT) could be valuable for early detection of abnormalities in collagen and elastic fibers and ectopic calcifications in suspected PXE individuals and for patient follow-up [8,9].

OCT is based on the principles of Michelson interferometry. It uses an optical probe to direct a light beam from a broad-bandwidth light source, typically around 1300 nm, through a beam splitter into both a sample arm and a reference arm. The reflected light is then sent back to the interferometer for detection, where interference fringes are observed when the optical path length from the sample arm matches the short coherence length of the reference arm's laser [10]. OCT provides in vivo, two-dimensional, cross-sectional en-face images of skin areas covering several square millimeters, with a penetration depth of up to 1.5 mm and a spatial resolution between 3 and 15 µm [11]. High-definition OCT enables visualization even of individual cells [12]. Another technique, named dynamic OCT (D-OCT), also detects motion in the OCT images and can reveal both tissue structure and blood vessel morphology by capturing changes between consecutive frames [11].

Objective

The study aimed to validate D-OCT as a noninvasive diagnostic tool for detecting PXE-related abnormalities in dermal tissue.

Methods

Design and Settings

This case-control study was conducted at the Neurocutaneous Rare Diseases Center of Umberto I Policlinic (Rome, Italy). We enrolled all patients with a definitive diagnosis of PXE, established according to the criteria proposed by Plomp et al. [5] who attended our outpatient clinic from

May 2023 to September 2024 and agreed to participate in the study. Controls comprised individuals who voluntarily underwent general dermatology examinations for oncological prevention (mole check-up) during the same period, with no preexisting severe dermatological condition.

Written informed consent was obtained from all participants, and the study adhered to the principles outlined in the Declaration of Helsinki, good clinical practice guidelines, and all applicable laws and regulations.

Patient Evaluation

Dermatological Evaluation

All patients underwent dermatological evaluation of the lateral cervical, retrocervical, axillary, and periumbilical regions. To minimize variability due to potential asymmetries and to ensure a consistent and standardized assessment, only the left sides of the lateral cervical and axillary folds were examined.

Clinically, each fold was scored using a 4-point scale ranging from 0 to 3:

0: no cutaneous sign

1: presence of papules

2: presence of confluent papules or plaques

3: skin laxity and wrinkles

No intermediate grades were assigned.

Instrumental Evaluation

A VivoSight Dx multi-beam OCT dermatological scanner (manufactured by Michelson Diagnostics Ltd., Kent, UK) equipped with proprietary D-OCT imaging software was used to evaluate all the aforementioned anatomical sites. The optical resolution of the scanner is 7.5 µm laterally and 5 µm axially, providing clear visualization of skin morphology and fine blood vessels. The probe offers a field of view of 6 mm x 6 mm and an imaging depth ranging from 1.0 to 2.0 mm. Additionally, the handheld probe features a color camera to facilitate accurate lesion placement and provide contextual images. No skin preparation, such as gel application, was necessary [13].

Data Analysis

D-OCT images were examined focusing on collagen and elastic fibers and vessels. For fiber analysis, an automatic software, namely OCT attenuation coefficient, provided two parameters: density coefficient and attenuation coefficient. For vascular analysis, images acquired at depths of 300 µm and 500 µm were processed using graphic reprocessing software (ImageJ), which provided vessel density measurements at these specific depths.

Descriptive statistics (mean, median, standard deviation) were employed to synthesize the data, and correlations were determined using Spearman's ρ. To identify differences between patients and controls, the non-parametric Mann-Whitney U test was utilized, with a significance level set at $P<0.05$.

Results

A total of 23 patients with PXE and 11 healthy controls were included in the study. The mean age of the PXE patients was 46.39 years (standard deviation: 15.91), with five males (21.74%) and 18 females (78.26%) (Table S1). The control group had a mean age of 46.72 years (standard deviation: 16.78), with four males (27.27%) and seven females (72.73%).

Cutaneous involvement was observed in 21 of the 23 PXE patients (91.30%). The most frequently affected site was the retrocervical fold, involved in 20 patients (86.95%), followed by the lateral cervical fold in 19 patients (82.60%), the axillary region in 12 (52.17%), the inguinal fold in nine (39.13%), and the cubital fold in five patients (21.74%). Notably, no clinical alterations were detected in the periumbilical region (Table 1).

Analysis of fiber characteristics revealed a statistically significant positive correlation between clinical severity (graded on a 0–3 scale) and the fiber density coefficient, measured via D-OCT, specifically in the retrocervical fold, the most frequently affected area in this cohort (Spearman's $\rho=0.507$; $P=0.014$). However, this correlation was less pronounced in patients with milder clinical manifestations (severity index <2), as shown in Figure 1.

When comparing PXE patients with healthy controls, significant differences in fiber density and attenuation were observed across all examined anatomical sites (Figure 2), except for axillary region (Table 2). It should be noted that the p-value for attenuation in the periumbilical region appeared as 0.05 due to rounding; however, the actual value was slightly below 0.05, thus fulfilling the criterion for statistical significance. Overall, PXE patients demonstrated lower fiber density values (ranging from 82.89% to 88.04%) and higher attenuation values (ranging from 114.53% to 138.21%) compared to controls.

Table 1. Number of PXE patients showing cutaneous involvement in the anatomical regions examined.

Region	Patients (N)	Percentage (%)
Retrocervical fold	20	86.95%
Left lateral cervical fold	19	82.60%
Left axillary fold	12	52.17%
Inguinal fold	9	39.13%
Cubital fold	5	21.74%
Periumbilical fold	0	0.00%

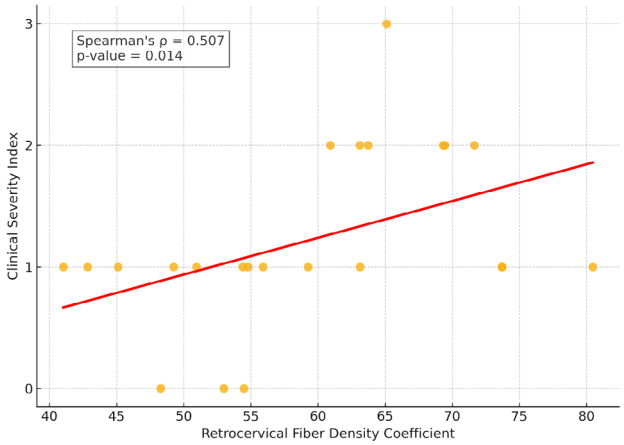

Figure 1. A positive statistically significant correlation was observed between the retrocervical fiber density coefficient and the clinical severity index (Spearman's ρ=0.507; *P*=0.014), as illustrated by the red regression line. This association appeared more consistent in patients with moderate-to-severe clinical involvement (severity index ≥2), whereas values were more scattered among those with milder manifestations (severity index <2).

Regarding vascular parameters, D-OCT assessments at depths of 300 µm and 500 µm revealed no significant correlation with clinical severity, nor significant differences between patients and controls, except at 500 µm depth in the axillary region (Figure 3). At this level, vessel representation was nearly 2.5 times lower in PXE patients compared to controls (3479.83 vs. 8599.73), as detailed in Table 3.

Discussion

Pseudoxanthoma elasticum is a rare genetic metabolic disorder in which dermal changes often manifest earliest and most prominently in friction-prone flexural areas. In line with previous studies, the retrocervical, lateral cervical, and axillary regions were among the most affected in our cohort, while the periumbilical area, less subject to mechanical stress, was typically spared (Table 1) [4,6].

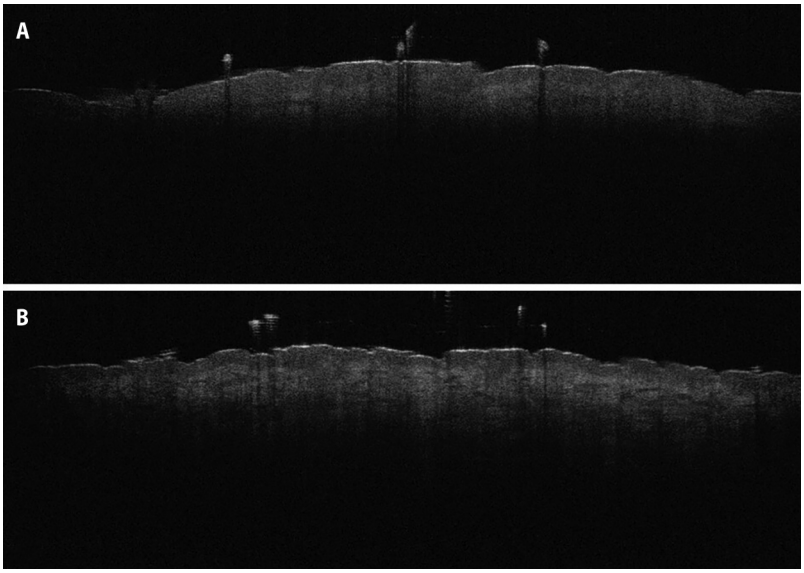

Figure 2. D-OCT images of (A) the left lateral cervical region in a PXE patient and (B) a control. In the PXE patient, the upper dermis exhibits decreased reflectivity and a more heterogeneous structure compared to the control. Quantitative analysis highlights a significant reduction in collagen density, along with noticeable disorganization of elastic fibers (refer to Table 2 for details).

Table 2. Mean Fiber Density and Attenuation Coefficients in PXE Patients and Controls, as Calculated using the OCT Attenuation Coefficient Software. All differences were statistically significant, except in the left axillary region.

	Retrocervical fold		Left lateral cervical fold		Left axillary fold		Periumbilical fold	
	Mean density	Mean attenuation	Mean density	Mean attenuation	Mean density	Mean attenuation	Mean density	Mean attenuation
Cases	59.29	0.0026	62.82	0.0025	63.15	0.0026	62.21	0.0024
Controls	71.53	0.0019	71.35	0.0019	70.33	0.0024	72.90	0.0021
Cases/Controls Ratio	82.89	138.21	88.04	132.40	89.79	107.55	85.34	114.53
P-value	0.00	0.00	0.01	0.00	0.19	0.12	0.00	0.05

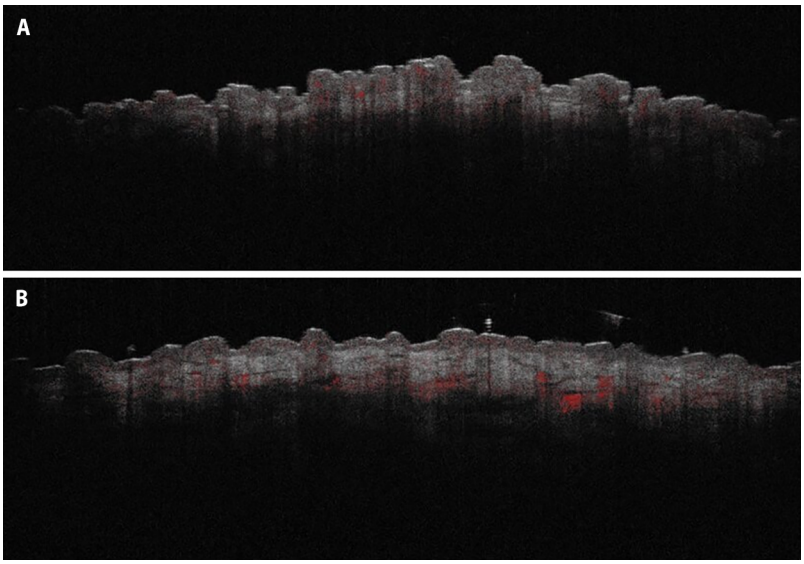

Figure 3. D-OCT images of (A) the left axillary fold in a PXE patient and (B) a control. In the PXE patient, vessel density is markedly reduced in this area, as confirmed by quantitative analysis (refer to Table 3 for details).

Table 3. Mean Vessel Density at 300 µm and 500 µm Depths in PXE Patients and Controls, analyzed using ImageJ Software. A statistically significant difference was observed only in the left axillary region at 500 µm depth.

	Retrocervical fold		Left lateral cervical fold		Left axillary fold		Periumbilical fold	
Average Vessel Density:	300 µm Depth	500 µm Depth	300 µm Depth	500 µm Depth	300 µm Depth	500 µm Depth	300 µm Depth	500 µm Depth
Cases	9923.39	21659.41	8330.91	16654.48	1487.52	3479.83	677.83	2488.91
Controls	7200.36	18064.00	11705.18	26030.55	1891.91	8599.73	611.55	3043.27
Cases/ Controls Ratio	137.82	119.90	71.17	63.98	78.63	40.46	110.84	81.78
P-value	0.61	0.11	0.42	0.80	0.21	0.00	0.91	0.66

Noninvasive techniques like D-OCT, which provides precise numerical data regarding fiber density, attenuation, and tissue vascularization, can effectively complement clinical assessments. In our study, D-OCT showed concordance with clinical findings, particularly in evaluating fiber density in the retrocervical region, the area most frequently involved (Figure 1). Conversely, in less frequently affected areas, or in cases of milder retrocervical involvement, this concordance tended to decrease. This is likely because D-OCT, being more sensitive, can detect minimal abnormalities that are not clinically visible. In fact, D-OCT revealed lower fiber density and higher attenuation even in the periumbilical region, despite the absence of clinical signs (Table 2).

A larger cohort may help to identify statistically significant differences in fiber parameters in additional areas, including the axillary folds, where p-values in the present study exceeded 0.05 (Table 2).

Given these findings, D-OCT may emerge as a valuable tool for the early, noninvasive diagnosis of PXE, potentially reducing the need for invasive procedures such as skin biopsy, which remains a useful diagnostic criterion [5]. For example, D-OCT could be used for rapid, painless screening of family members of PXE patients and could improve monitoring of disease progression by enhancing both sensitivity and specificity.

However, D-OCT encounters challenges in vascular assessment. No significant difference in vascular parameters was observed between PXE patients and controls, particularly at the 300 µm depth (Table 3). This may be explained by age-related vascular changes, such as increased stiffness, decreased density, and disorganized architecture [14], that affect both PXE patients and healthy individuals. Interestingly, at 500 µm depth, only in the axillary region, notable differences emerged. This could be because the deep histological alterations typical of PXE in the axilla may outweigh the effects of photoaging, which more heavily impacts other sun-exposed areas evaluated in this study [14].

Limitations

While this study included a relatively small sample size, it should be noted that it represents a pilot investigation into a rare disease, whose incidence is estimated to be between 1 in 25,000 and 1 in 100,000 individuals. Moreover, this is the first study to apply D-OCT in this specific context. Another limitation is that D-OCT does not clearly distinguish between elastic and collagen fibers, which may both be morphologically altered and calcified in PXE patients, particularly when their thickness falls below the optical resolution of the technique [5,7]. However, these histological changes indirectly influence D-OCT parameters, allowing for their measurement. Future studies with larger patient cohorts and more advanced technology will corroborate or contradict our findings.

Conclusion

D-OCT can identify dermal alterations in PXE patients, even in clinically unaffected areas. This technique offers a promising, sensitive, noninvasive diagnostic alternative to skin biopsies, with great potential for early detection and ongoing monitoring of the genetic disorder.

Ethical Issues: The authors warrant that any national or international law on human and environmental rights was not violated.

Ethics Statement: The patients in this manuscript have given written informed consent to publication of their case details.

Consent to Publish: The authors give the *Dermatology Practical & Conceptual Journal* the exclusive rights to publish their article, in whole or in part, in the aforementioned journal. The data that support the findings of this article are available from the corresponding author upon reasonable request.

References

1. Verschuere S, Navassiolava N, Martin L, Nevalainen PI, Coucke PJ, Vanakker OM. Reassessment of causality of ABCC6 missense variants associated with pseudoxanthoma elasticum based on Sherloc. Genet Med. 2021 Jan;23(1):131–9. DOI: 10.1038/s41436-020-00945-6. PMID: 32873932.
2. Verschuere S, Van Gils M, Nollet L, Vanakker OM. From membrane to mineralization: the curious case of the ABCC6 transporter. FEBS Lett. 2020 Dec;594(23):4109–33. DOI: 10.1002/1873-3468.13981. PMID: 33131056.
3. Bisaccia F, Koshal P, Abruzzese V, Castiglione Morelli MA, Ostuni A. Structural and functional characterization of the abcc6 transporter in hepatic cells: Role on pxe, cancer therapy and drug resistance. Int J Mol Sci. 2021;22(6):1–12. PMID: 33799762.
4. Germain DP. Pseudoxanthoma elasticum. Orphanet J Rare Dis. 2017 May;12(1). DOI: 10.1186/S13023-017-0639-8. PMID: 28486967.
5. Plomp AS, Toonstra J, Bergen AAB, Van Dijk MR, De Jong PTVM. Proposal for updating the pseudoxanthoma elasticum classification system and a review of the clinical findings. Am J Med Genet A. 2010 Apr;152(4):1049–58. DOI: 10.1002/ajmg.a.33329. PMID: 20358627.
6. Laghi A, Mandel VD, Zubba I, Franceschini C, Demofonte I, Chello C, et al. Comprehensive analysis of pseudoxanthoma elasticum: epidemiological, genetic, and clinical findings from the leading Italian center. Italian journal of dermatology and venereology. 2024 Aug;159(4):430–5. DOI: 10.23736/S2784-8671.24.07949-0. PMID: 39069841.
7. Neidner KH. Pseudoxanthoma elasticum. Clin Dermatol. 1988;6(1):1–4. DOI: 10.1016/0738-081x(88)90003-x. PMID: 3359381.
8. Persechino F, Giordano D, Marini CD, Franceschini C, Ardigò M, Persechino S. Dermoscopy, Optical Coherence Tomography, and Histological Correlation of Pseudoxanthoma Elasticum. Dermatol Pract Concept. 2019 Jul;9(3):209–10. DOI: 10.5826/dpc.0903a07. PMID: 31384495.
9. Mehrabi JN, Doong J, Lentsch G, Mesinkovska N. Imaging of vivo pseudoxanthoma elasticum via multiphoton microscopy and optical coherence tomography. JAAD Case Rep. 2020 Aug;6(8):702–4. DOI: 10.1016/j.jdcr.2020.05.029. PMID: 32715054.
10. Csuka EA, Ward SC, Ekelem C, Csuka DA, Ardigò M, Mesinkovska NA. Reflectance Confocal Microscopy, Optical Coherence Tomography, and Multiphoton Microscopy in Inflammatory Skin Disease Diagnosis. Lasers Surg Med. 2021 Aug;53(6):776–97. DOI: 10.1002/lsm.23386. PMID: 33527483.
11. Schuh S, Holmes J, Ulrich M, Themstrup L, Jemec GBE, De Carvalho N, et al. Imaging Blood Vessel Morphology in Skin: Dynamic Optical Coherence Tomography as a Novel Potential Diagnostic Tool in Dermatology. Dermatol Ther (Heidelb). 2017 Jun;7(2):187–202. DOI: 10.1007/s13555-017-0175-4. PMID: 28258554.
12. Lindsø Andersen P, Olsen J, Friis KBE, Themstrup L, Grandahl K, Mortensen OS, et al. Vascular morphology in normal skin studied with dynamic optical coherence tomography. Exp Dermatol. 2018 Sep;27(9):966–72. DOI: 10.1111/exd.13680. PMID: 29733465.
13. VivoSight brochure [Internet]. [cited 2025 Jan 1]. Available from: https://vivosight.com/wp-content/uploads/2023/03/VivoSight-brochure_2023.pdf
14. Bentov I, Reed MJ. The effect of aging on the cutaneous microvasculature. Microvasc Res. 2015 Jul;100:25–31. DOI: 10.1016/j.mvr.2015.04.004. PMID: 25917013.